Electrical properties of GeSe₂-Sb₂Se₃-PbTe thin films

B. STEFANOVA[a], D. NESHEVA[a*], K. PETKOV[b], M. RADONOVA[c], G. VASSILEV[c], V. VASSILEV[c]

[a]Institute of Solid State Physics, Bulgarian Academy of Sciences, 72 Tzarigradsko Chaussee Blvd., 1784 Sofia, Bulgaria.
[b]Institute of Optical Materials and Technologies, Bulgarian Academy of Sciences, Acad. G. Bonchev str., bl. 109, 1113 Sofia, Bulgaria.
[c]Dapartment of Non-Ferrous Metals and Semiconductor Technologies, University of Chemical technology and matalurgy, 8 Kl. Ohridski blvd, 1756 Sofia, Bulgaria

Thin films from $(GeSe_2)_x(Sb_2Se_3)_y(PbTe)_z$ ($x+y+z$=100 %) have been prepared by thermal evaporation of preliminary synthesized glassy material. Energy-dispersive X-ray spectroscopy has been applied for determination of the film composition. Temperature measurements of the electrical conductivity in the range 20-110 °C have also been carried out. It has been found that the room temperature dark conductivity varies within six orders of magnitude (10^{-9}-10^{-3} S/cm) with changing the film composition. It has also been shown that the dark current thermal activation energy does not depend of the applied electric field which implies that electrical polarization does not occur and the activation energy of the dark current indicates the position of the Fermi-level in the gap. A strong decrease of the activation energy has been observed with increasing the molar percentages of both PbTe and Sb₂Se₃. The comparison of the optical band gap with the double-dark current activation energy has implied that only the films that not contain PbTe are amorphous while all films containing PbTe are nanocrystalline.

1. Introduction

Amorphous chalcogenide films can be fabricated over large areas by inexpensive deposition techniques and are easy to handle. They show a unique set of photoinduced effects which makes them very interesting for optical fabrication and performance [1]; e.g., the optical band gap and the refractive index can be effectively modified by illumination. Using photo-induced effects, optical elements for applications in communications, interconnections, and data storage have been patterned in chalcogenide glasses simply by illumination. These materials show high transmission in the infrared region of the spectrum and therefore they attract much attention for development of active and passive IR devices.

Non-volatile memories are useful elements of integrated circuits due to their ability to maintain data without a power supply. A great variety of chalcogenide alloys form a class of programmable phase change materials. The use of phase-change chalcogenide alloy films for electrical and optical information storage was first reported in 1968 [2] and in 1972 [3], respectively. The memory technology is based on an electrically initiated, reversible rapid amorphous-to-crystalline phase-change process in multicomponent chalcogenide alloy materials similar to those used in rewriteable optical disks (for a comprehensive review see [4]). A great variety of alloys such as GeSbTe, InSbTe, Te-Ge-Sb-S, Ge-Sb-Se-Te and many others have been suggested for use as active materials for this application [5-8].

Generally, the complication of the chemical composition and the structure of glasses increases the probability for observation of new properties, as a result of which the spectrum of possible application areas widens. Therefore, the number of the scientific publications aiming preparation and characterization of complex chalcogenide glasses is high [9 and reference therein].

In this study, electrical characterization of $(GeSe_2)_x(Sb_2Se_3)_y(PbTe)_z$ thin films ($x+y+z$=100 %) with seven different compositions, prepared by thermal vacuum evaporation of preliminary synthesized glassy materials, is carried out. For comparison PbTe single layers are also explored.

2. Experimental details

Glasses from $(GeSe_2)_x(Sb_2Se_3)_y(PbTe)_z$ (x = 36-80, y = 8-54, z = 0-40) with 7 different compositions (see Table 1) were synthesized by conventional melt quenching technique. The synthesis was performed with step-wise heating up to 500, 800 and 950 °C, at rates 3-4, 2-3 and 2-3°°C/min, respectively. Homogenizing annealing of the melts was carried out at these temperatures for 0.5, 0.5 and 2.0 h, correspondingly, combined with continuous vibration stirring at the highest temperature. The samples were quenched in ice cold water with cooling rate of 15 °C/sec. The glassy state was proven by visual, XRD and electron microscopy analyses [10].

Thin films (around 1 μm thick) were prepared by thermal evaporation of preliminary synthesized and powdered glasses in a high vacuum of 6×10^{-6} Torr, at evaporation rate in the range 1.5-2.5 nm/s. The composition of both bulk samples and thin films was determined by energy dispersive X-ray spectroscopy (EDS) using a scanning electron microscope with a X-ray microanalyser Jeol Superprobe 733 (Japan) operating at an electron accelerating voltage of 20 kV and a current of 1.4 nA. The layers for the composition and surface morphology measurements were deposited on crystalline

silicon substrate while those for the electrical measurements were prepared on glass substrates. The EDS results have shown (Table 1) that the film compositions demonstrate some deviation from the composition of bulk samples due to the process of thermal evaporation. In the paper below the composition of the respective source glass is used for the film labelling.

The surface morphology of the films was studied by means of a Scanning Electron Microscope (SEM) Philips SEM 515 operating in regime of secondary electrons (SEI) and at an accelerating voltage of 20 kV. The angle between the electron beam and the perpendicular to the film surface was varied between 0 and 40 deg. The layers for the composition and surface morphology measurements were deposited on crystalline silicon substrate.

Dark current dc measurements were carried out using sputtered gold electrodes on the top surface of the layers which produce a gap cell with an active area of $1 \times (3\text{-}5)$ mm^2. Temperature dependences of the dark current were measured in the 20-110 ^{o}C range at a heating rate of 0.04 ^{o}C/sec. The applied temperatures are well below the glass transition temperatures of all compositions studied [10].

3. Results and discussion

Current-voltage characteristics measured at applied electric fields in the range 1-10^3 V/cm are depicted in Fig. 1. As seen they are Ohmic-like in the whole range of the applied fields. This result is important for correct determination of the film conductivity and its activation energy as well as for the reliability of the conclusions made on its basis.

The variation of the room temperature dark conductivity with the film composition is shown in Fig. 2. One can see that the dark conductivity varies within six orders of magnitude (10^{-9}-10^{-3} S/cm). Such strong variation cannot be easily achieved for binary or ternary chalcogenides with an electronic conductivity and may be useful for various applications.

In order to exclude a possible influence of the electrical polarization, observed in highly resistive films, on the determined activation energy, temperature dependences of the dark current were measured by applying five different electric fields. In Fig. 3 a series of such temperature dependences measured on a (GeSe$_2$)$_{72}$(Sb$_2$Se$_3$)$_{18}$(PbTe)$_{10}$ film is shown in semi-log coordinates.

Table 1 Source glass and film compositions determined by EDS measurements

| No	Bulk glasses (mol. %)	Bulk glasses (at. %)	Thin films (at. %)
1	(GeSe$_2$)$_{80}$(Sb$_2$Se$_3$)$_{20}$	Ge$_{23.5}$Sb$_{11.8}$Se$_{64.7}$	Ge$_{13.6}$Sb$_{25.6}$Se$_{60.8}$
2	(GeSe$_2$)$_{82}$(Sb$_2$Se$_3$)$_8$(PbTe)$_{10}$	Ge$_{26.8}$Sb$_{5.2}$Se$_{61.4}$Pb$_{3.3}$Te$_{3.3}$	Ge$_{27.2}$Sb$_{6.3}$Se$_{58.5}$Pb$_{1.0}$Te$_{7.0}$
3	(GeSe$_2$)$_{72}$(Sb$_2$Se$_3$)$_{18}$(PbTe)$_{10}$	Ge$_{22.1}$Sb$_{11.0}$Se$_{60.7}$Pb$_{3.1}$Te$_{3.1}$	Ge$_{16.4}$Sb$_{17.8}$Se$_{58.8}$Pb$_{7.0}$
4	(GeSe$_2$)$_{54}$(Sb$_2$Se$_3$)$_{36}$(PbTe)$_{10}$	Ge$_{14.9}$Sb$_{19.8}$Se$_{59.7}$Pb$_{2.8}$Te$_{2.8}$	Ge$_{8.0}$Sb$_{32.0}$Se$_{54.3}$Pb$_{1.7}$Te$_{4.0}$
5	(GeSe$_2$)$_{36}$(Sb$_2$Se$_3$)$_{54}$(PbTe)$_{10}$	Ge$_{9.1}$Sb$_{27.1}$Se$_{58.8}$Pb$_{2.5}$Te$_{2.5}$	Ge$_{3.4}$Sb$_{39.4}$Se$_{53.0}$Pb$_{1.2}$Te$_{3.0}$
6	(GeSe$_2$)$_{56}$(Sb$_2$Se$_3$)$_{14}$(PbTe)$_{30}$	Ge$_{18.8}$Sb$_{9.4}$Se$_{51.7}$Pb$_{10.0}$Te$_{10.0}$	Ge$_{15.0}$Sb$_{15.6}$Se$_{48}$Pb$_{11.6}$Te$_{10.0}$
7	(GeSe$_2$)$_{48}$(Sb$_2$Se$_3$)$_{12}$(PbTe)$_{40}$	Ge$_{16.9}$Sb$_{8.5}$Se$_{46.5}$Pb$_{14.0}$Te$_{14.0}$	Ge$_{16.8}$Sb$_{9.0}$Se$_{45.2}$Pb$_{17.0}$Te$_{12.0}$
8	PbTe	Pb$_{50}$Te$_{50}$	Pb$_{46.1}$Te$_{53.9}$
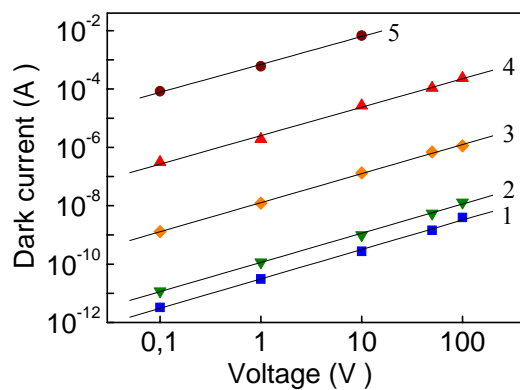
Fig. 1. Current-voltage characteristics of five films. The numbers correspond to the following compositions:1 - (GeSe$_2$)$_{82}$(Sb$_2$Se$_3$)$_8$(PbTe)$_{10}$;
2 - (GeSe$_2$)$_{54}$(Sb$_2$Se$_3$)$_{36}$)(PbTe)$_{10}$;
3 - (GeSe$_2$)$_{36}$(Sb$_2$Se$_3$)$_{54}$)(PbTe)$_{10}$;
4 - (GeSe$_2$)$_{48}$(Sb$_2$Se$_3$)$_{12}$)(PbTe)$_{40}$; 5 – PbTe.
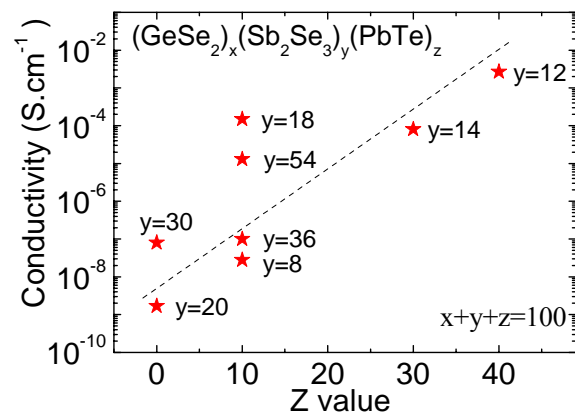*The solid lines represent linear fits of the experimental points (symbols).*

Fig. 2. Variation of the room temperature dark conductivity with the variance of the mol. % of the PbTe fraction (z). The mol. % of the Sb$_2$Se$_3$ (y) fraction is denoted near each experimental point and one should keep in mind that x+y+z = 100 %. The dashed line is guide to the eye.

The observed linearity of all dependences measured indicates that in all samples the dark current I obeys the relation

$$I \sim \exp(-E_d/kT) \qquad (1)$$

in which E_d is the dark current activation energy, k – Boltzman constant and T – measuring temperature.

Similar series of curves have been taken for all other compositions which give as basis to conclude that the dark current thermal activation energy is not affected by the applied electric field.

It is known [11] that at high enough temperature (normally $T > 20\ ^oC$) the conduction process in amorphous materials changes from hopping transport in localized band tail states to conduction by carriers in extended states and the conductivity changes with temperature are described by the relation (for electrons) [11]

$$\sigma = \sigma_{\min} \exp(E_c - E_F)/kT \qquad (2)$$

where E_c is the conduction band mobility edge, E_F is the Fermi level position and $\sigma_{\min}$ is the minimum metallic conductivity. Since the measuring temperatures used in this study are quite high one can assume that in the films studied transport of carriers in extended state takes place, most likely transport of holes in the valence band. Hence, the activation energy determined gives information about the Fermi-level position in the gap.
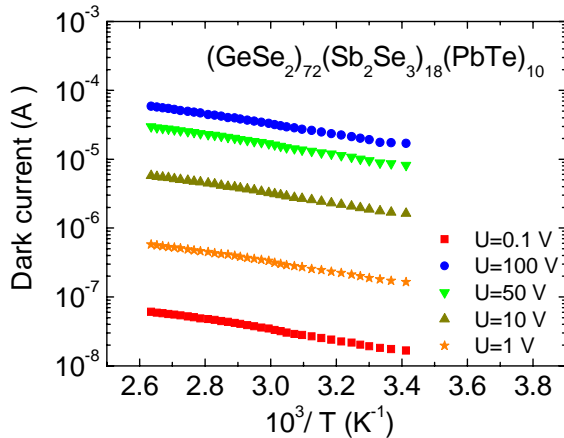
Fig. 3. Temperature dependences of the dc dark current through a $(GeSe_2)_{72}(Sb_2Se_3)_{18}(PbTe)_{10}$ thin film measured at different applied voltages denoted in the figure.

Fig. 4 shows the dark current activation energy versus molar % of PbTe, z. A strong decrease of the activation energy, from 0.7 eV for the $(GeSe_2)_{80}(Sb_2Se_3)_{20}$ film ($z = 0$) to less than < 0.1 eV for the film with $z = 40$ mol. % PbTe, is observed with increasing PbTe molar percentage. Besides, a careful consideration of the E_d changes in the four samples with $z = 10$ mol. % PbTe shows that the increase of the Sb_2Se_3 mol. % from $y = 8$ to 54 mol. % also causes an E_d decrease. Thus, by varying either y or z one can successfully change both the $(GeSe_2)_x(Sb_2Se_3)_y(PbTe)_z$ films conductivity and its activation energy. Further studies are necessary to find

a way for changing the electrical properties of the $(GeSe_2)_x(Sb_2Se_3)_y(PbTe)_z$ films in a controllable manner.

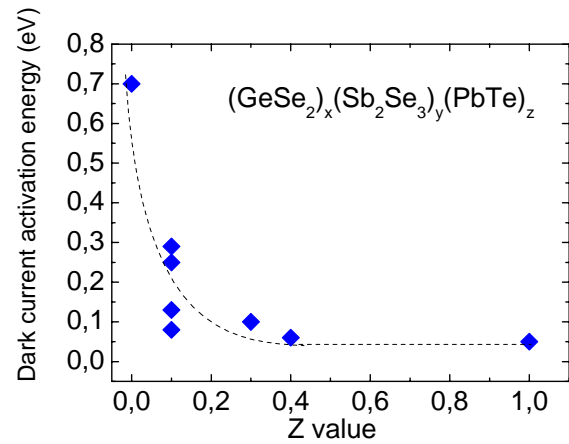*Fig. 4. Variation of the dark current activation energy E_d with the variance of the mol % of the PbTe fraction in the complex $(GeSe_2)_x(Sb_2Se_3)_y(PbTe)_z$ alloys. The y-values are the same as those written in Fig. 2. The dashed line is guide to the eye.*

The density of electron states remains a valid concept for non-crystalline as for crystalline materials [11]. A principal feature of this concept in non-crystalline materials is the existence of 'mobility edges' which are identified with the critical energies separating localized states from extended states. The difference between the energies of the mobility edges in the valence and conduction bands is called the 'mobility gap'. A model for the location of the Fermi level near mid-gap in amorphous semiconductors, based on potential fluctuations of an 'electrostatic' nature fluctuations, has been suggested by Fritzsche [12] and based on this model $E_F - E_V$ (E_V - the valence band mobility edge) is expected to be approximately half the optical band gap E_g^o. Hence the double-dark current activation energy $(2E_d)$ value gives the mobility gap which should be close to the optical band gap. A comparison of $2E_d$ with the optical band gap of our films is shown in Fig. 5. One can see that with an exception (the $(GeSe_2)_{80}(Sb_2Se_3)_{20}$ film) the optical band gap energy is much higher than $2E_d$. This implies that only the films with $z = 0$ (not containing PbTe) and relative low $y = 20$ display a behavior that is typical for amorphous films. The $2E_d$ of all films containing PbTe is much smaller than the optical band gap energy. This observation can be understood if one assumes that those films are microcrystalline rather than amorphous.

Fig. 6 shows the SEM micrograph of a $(GeSe_2)_{36}(Sb_2Se)_{54}(PbTe)_{10}$ thin film. Similar images have been obtained for the surface morphology of films with other compositions. As seen from the figure, the film surface is quite smooth and at this resolution no grains larger than 100 nm are distinguished. Hence, based on the electrical and SEM data one can conclude that the films containing PbTe are nanocrystalline rather than amorphous.
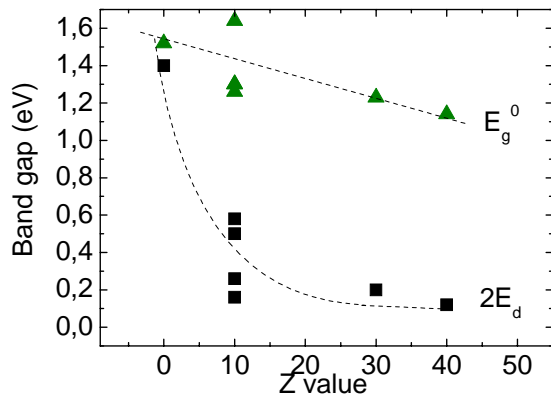
Fig. 5. Changes of the optical band gap E_g^o[13] and double-dark current activation energy ($2E_d$) of $(GeSe_2)_x(Sb_2Se_3)_y(PbTe)_z$ thin films with changing the PbTe mol. %. The dashed lines are guide to the eye.
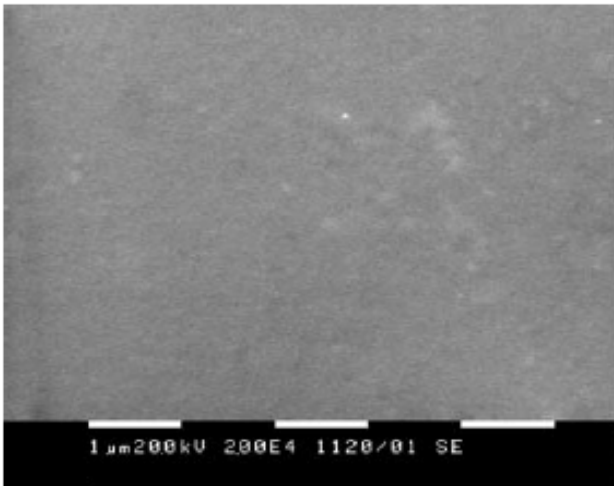

Fig. 6. SEM image of a $(GeSe_2)_{36}(Sb_2Se_3)_{54}(PbTe)_{10}$ thin film.

4. Conclusions

Electrical properties and surface morphology of thin films from $(GeSe_2)_x(Sb_2Se_3)_y(PbTe)_z$ ($x+y+z = 100$ %) have been investigated. Temperature measurements of the electrical conductivity carried out at $T > 20$ °C have revealed a strong change of the room temperature dark conductivity; it varies within six orders of magnitude (10^{-9}-10^{-3} S/cm) with changing the film composition. A strong decrease of the activation energy has been observed with increasing the molar percentages of both PbTe and Sb_2Se_3 indicating a significant shift of the Fermi-level to the valence band. Based on the comparison of the optical band gap with the double-dark current activation energy and SEM data a conclusion has been made that only the films that not contain PbTe are amorphous while all films containing PbTe are nanocrystalline.

References

[1] A. Zakery, S. R. Elliott, J. Non-Cryst. Solids **330**, 1 (2003).
[2] S. R. Ovshinsky, Phys. Rev. Lett. **21**, 1450 (1968).
[3] J. Feinleib, J. de Neufville, S. C. Moss, S. R. Ovshinsky, Appl. Phys. Lett. **18,** 254 (1971).
[4] S. Hudgens and B. Johnson, MRS Bulletin/November 2004, page 1.
[5] N. Yamada, K. Nagata, K. Nishiuchi, Sh. Furukawa, patent EP 0 899 725 A1, 1998.
[6] J. Liu, US patent 7,560,723 B2, July 2009.
[7] J. Liu, US patent 7,638,357 B2, Dec. 2009.
[8] H-L. Lung, US patent 7,932,101 B2, Apr. 2011.
[9] V. Vassilev, G. Vassilev, J. Dikova, K. Petkov, J. Optoelectron. Adv. Mater. **11**, 2024 (2009).
[10] V. Vassilev, M. Radonova, S. Boycheva, E. Fidancevska, Optoel. Adv. Mat. (2011), in press.
[11] N. Mott, E. A. Davis, Electronic Processes in Non-Crystalline Materials, Clarendon Press, Oxford, 1979.
[12] H. Fritzsche, J. Non-Cryst. Solids **6**, 49 (1971).
[13] K. Petkov, J. Tasseva, V. Vassilev, L. Aljihamani, J. Optoelectron. Adv. Mater. (2011), in press.

[*]Corresponding author: nesheva@issp.bas.bg